Orbital: The Electronic Journal of Chemistry
journal homepage: www.orbital.ufms.br
e-ISSN 1984-6428

| Vol 12 | | No. 3 | | July-September 2020 |

FULL PAPER

Electrochemical and Theoretical Studies on the Artesunate Reduction

Audrey B. Silva[a], Charles L. Brito[b], Gustavo H. G. Trossini[b], Mauro A. La-Scalea[a*]

[a]Departamento de Química, Instituto de Ciências Ambientais, Químicas e Farmacêuticas Universidade Federal de São Paulo, Diadema, SP, Brasil.
[b]Departamento de Farmácia, Faculdade de Ciências Farmacêuticas, Universidade de São Paulo, São Paulo, SP. Brasil.

Article history: Received: 22 October 2019; revised: 10 August 2020; accepted: 11 August 2020. Available online: 23 September 2020. DOI: http://dx.doi.org/10.17807/orbital.v12i3.1439

Abstract:

Malaria is the most devastating tropical disease in the world and this scenario is worsened by the absence of effective treatment. However, the plasmodium resistance to artemisinin does not show clinical relevance. The drug mechanism of action is associated to the endoperoxide moiety breakage. Artesunate is a semi-synthetic derivative of artemisinin and its absorption is facilitated due to its higher solubility in water. As a sesquiterpene lactone, artesunate can be electrochemically reduced in aqueous media on the glassy carbon electrode, having been studied by cyclic voltammetry, square wave voltammetry and chronoamperometry. The artesunate voltammetric reduction is diffusion-controlled and significantly irreversible. Its reduction is pH-independent, but from pH = 6.0 the cathodic current values increase in alkaline media, indicating that the proton-equilibrium occurs after the electron transfer step. The αn values calculated vary from 0.30 to 0.37, leading to the 0.0975 s^{-1} value for k_s. From the chronoamperometric data, two electrons (1.9 ± 0.4) are involved in the reduction process, being confirmed by the exact number of electrons obtained for artemisinin (1.9 ± 0.2). According to these results and computational findings, both drugs have the same reduction mechanism with the breakage of the endoperoxide bridge and consequent diol-derivative formation followed by the deoxy analog stabilization through the existence of a set of reactions involving protonation and charge transfer steps on the electrode surface.

Keywords: artesunate; artemisinin; electrochemical; endoperoxide bridge; irreversible reduction; LUMO-HOMO

1. Introduction

Malaria, a neglected tropical disease (NTD), is the most devastating worldwide and this scenario is worsened by the absence of effective treatment. Malaria is caused by protozoa belonging to five species of the genus *Plasmodium* and it is transmitted to humans through female *Anopheles* mosquitoes bites. In Latin America, around 250 thousand people are infected by *Plasmodium falciparum*. Although around half of the world population is at risk, the scale-up of interventions has been helping to reduce the global mortality rate by 37% in the last 15 years. In spite of these advances, the scenario remains alarming since there were an estimated 214 million cases of malaria and 438,000 deaths in 2015 [1].

Tropical diseases continue to represent a serious social problem, since adequate drug treatment is still lacking. Even so, the efforts in research and development (R&D) by the companies are too weak concerning a potential return to produce new therapies to invest significantly in the field [2, 3]. In this context, malaria is part of the group of 17 diseases that typically affect poor people in tropical countries [3, 4]. Current initiatives driven at R&D of NTDs are being led predominantly by the governmental, inter-governmental and private not-for-profit sectors implemented by means of public-private partnerships [5, 6]. An important example of these initiatives was the consortium founded by DND*i* and TDR in 2002, in which the Brazilian government took part involving the pharmaceutical company Farmanguinhos/

*Corresponding author. E-mail: mauro.scalea@unifesp.br

Fiocruz [7]. This initiative generated an important alternative for malaria treatment, the artesunate-mefloquine (MEFAS) [8].

MEFAS [8] is a salt derived from two antimalarial molecules, artesunate and mefloquine, and results have demonstrated that this new compound is more effective against malaria than the simple combination between the two original drugs. It is worth mentioning that the association of artesunate plus mefloquine hydrochloride has been adopted as first-line agents for uncomplicated malaria [9].

Both antimalarial drugs act as blood schizontocides [9, 10]. The action mechanism of mefloquine is still unknown, but it can be related with processes involving oxidative stress [11], while the action mechanism of artesunate follows the same recommended for artemisinin, in which the endoperoxide bridge under the attack of a reducing agent, like a ferrous ion, undergoes a rapid and effective cleavage [9].

Artemisinin (Figure 1A) is a sesquiterpene lactone containing a peroxide bridge responsible for its action mechanism [9]. Its semi-synthetic derivative, artesunate (Figure 1B), presents higher solubility in water, which provides an advantage over artemisinin, because its absorption is facilitated and artesunate can be formulated in oral, rectal, intramuscular, and intravenous preparations.

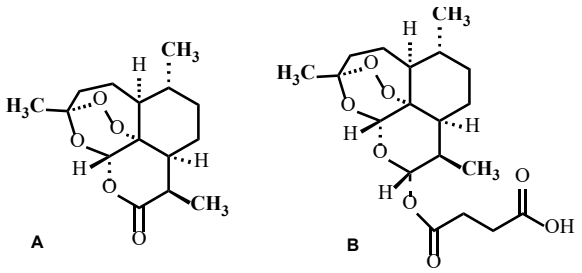

Figure 1. Molecular structures of artemisinin (A) and artesunate (B).

The pharmacological activities of drugs based on the charge transfer processes is an interesting research field for the study of physicochemical parameters having electrochemistry as technique applied. Electrochemical techniques are useful tools for the mechanism elucidation of drugs whose own redox steps are associated to the biological action processes, involving the identification of oxidation-reduction products and metabolite formation, as well as the acquisition of parameters used in studies of structure-activity relationships for drug design [12, 13]. Additionally, molecular modelling techniques are powerful tools successfully used to analyze and interface medicinal chemistry studies with electrochemical experimental results. These techniques association can significantly contribute to comprehend and elucidate the medicinal chemistry challenges, such as predicting biological activity and understanding drug action mechanisms [14].

Artemisinin can be chemically or electrochemically reduced, involving the endoperoxide bridge cleavage [15]. The cyclic voltammetric profile indicates an irreversible reduction with a little defined cathodic peak and with a high negative potential value [16-24]. Some derivatives like dihydroartemisinin [19], arteether [25], artemeter [26] and artesunate [20, 27] present similar voltammetric behavior similar to that of the original drug.

Additionally, the electrochemical techniques, mainly the cyclic voltammetry, have been applied in studies involving the interaction between artemisinin and its derivatives with heme group. The artemisinin reduction occurs with the cleavage of endoperoxide bridge catalyzed by the iron ions [9, 28]. The voltammetric behavior of artemisinin is significantly altered in the hemin presence, provoking anticipation of the cathodic peak for more positive potential values and increase on the peak current as well [16, 19-21, 23]. Studies with holotransferrin [29,30] and carbon nanofiber electrode functionalized with hemoglobin [31] registered analogous electrocatalytic behavior on the artemisinin. As artesunate presents structural similarity, the same mechanism is also observed [20].

Although artesunate is important in the therapeutics against malaria and its biological action associated with redox process, there have been few works published about artesunate reduction mechanism in detailed form. In this sense, this paper seeks to address a study on the artesunate electrochemical behavior in aqueous media using a glassy carbon electrode by applying cyclic voltammetry, square wave voltammetry and chronoamperometry. Moreover,

a computational study is performed clarifying the involved redox process. The system reversibility, effect of pH and electrode mechanism reaction are evaluated. The determination of the exact number of electrons is carried out through the chronoamperometric record for artesunate and artemisinin using the Cottrell equation, having the diffusion coefficient predicted by Wilke-Chang equation. A reduction mechanism is presented.

2. Results and Discussion

Several works on the electrochemical reduction of artemisinin and derivatives had been established with voltammetric measurements in non-aqueous or mixed media [16, 18-21, 26, 29-31]. Nevertheless, previous results [23] registered the possibility of the artemisinin voltammetric reduction in buffered-aqueous medium. This work aims to study the artesunate reduction only in aqueous media. However, initially cyclic voltammograms were obtained in mixed media, as depicted in Figure 2.

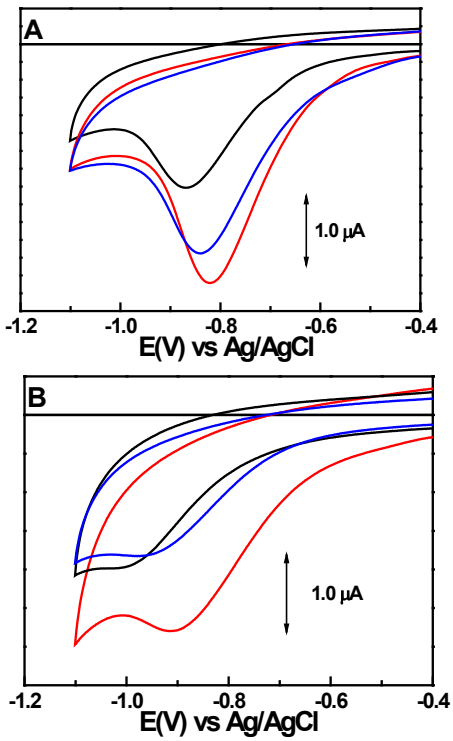

Figure 2. Cyclic voltammogramsof 0.1 mmol L^{-1} of (A) artemisinin and (B) artesunate in (—) buffer BR pH 6.0; (—) 20% methanol + buffer BR pH 6.0; (—) 20% acetonitrile + buffer BR pH 6.0. Scan rate = 0.10 V s^{-1}.

As it can be observed for both drugs the cyclic voltammograms registered only a single irreversible reduction wave at GCE, since there is no register in the reverse scan and being the higher values of current obtained in buffer BR pH 6.0. The artemisinin voltammetric reduction occurs in potential lightly less positive (-0,820 V) than that observed for artesunate (-0,906 V). Moreover, the voltammograms for the former showed better definition than that registered for the latter.

Peak potential values (Ep_c) for the voltammetric reduction of artesunate are shifted for more negative potential values with the scan rate (ν) increased. Ep_c values vary linearly in function of the log ν, as it can be observed in Figure 3a, with a displacement around 200 mV per tenfold increase in scan rate, showing a process significantly irreversible. The αn value (n = electrons number and α = electron transfer coefficient) was calculated applying the equation for a totally irreversible mechanism, in which $Ep_{/2}$ is the potential where the current is at half peak value [32].

$$Ep_{/2}=Ep_c\pm\frac{47.7}{\alpha n}\ mV$$

The αn values vary from 0.37 to 0.30 for a scan rate range between 0.1 and 1.0 Vs^{-1}. Considering that two electrons can be involved in the artesunate voltammetric reduction [23], the average value calculated for α is 0.16, slightly lower than those registered for artemisinin [18, 23]. Based on this result, k_s, the rate constant of the electrochemical reaction (s^{-1}), can be estimated applying the method proposed by Laviron (1979), from the following equation [33]:

$$Ep_c=E^0+\frac{2.303RT}{\alpha nF}\log\left(\frac{RTk_s}{\alpha nF}\right)-\frac{2.303RT}{\alpha nF}\log\nu,$$

being R the gas constant (8.314 $JK^{-1}mol^{-1}$), T temperature (298 K), F the Faraday constant (96,485 C mol^{-1}) and E^0 the formal standard redox potential. Taking the calculated slope by the linear fit (-0.198) αn = 0.299 was obtained, which corroborates the data showed above. From the intercept (-1.185) of the plot in Figure 3a, the k_s can be obtained if E^0 is known. The E^0 value can be deduced by the extrapolation on the ordinate in the correlation between Ep_c *vs.* ν, considering ν = 0 [34]. As it can be observed in Figure 3b, Ep_c varies exponentially with the increase of the scan rate and its fitting curve can

suggest -0.774 V as value for E^0, indicating that the k_s value calculated is 0.0975 s^{-1}.

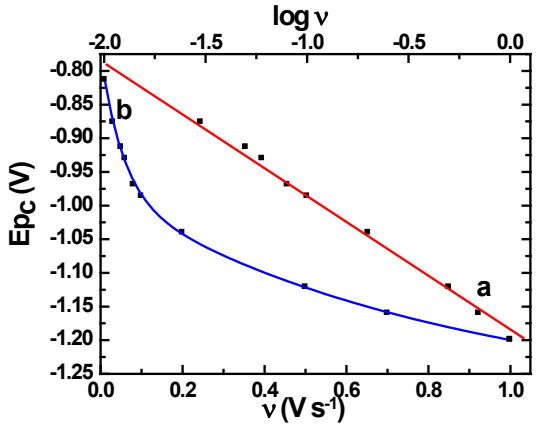

Figure 3. Influence of scan rate: (a) plot of Ep_c *vs.* log ν; (b) plot of Ep_c *vs.* ν. [Artesunate] = 1.0 mmol L^{-1} at pH = 6.0.

Figure 4 shows the influence of the scan rate variation on the cathodic peak current. The relationship between cathodic current values (Ip_c) and $\nu^{1/2}$ is linear, indicating that the electron transfer is controlled by diffusion. This behavior can be confirmed by the linear relationship obtained from the logarithm plot between peak current and scan rate for which a slope of 0.5 indicates a diffusion process [35]. In fact, the linear equation obtained shows a relatively close value for the slope (log Ip_c (μA)= 0.65 log ν (Vs^{-1}) + 0.74, R = 0.984, n = 8); between 0.01 and 1.0 Vs^{-1}. Therefore, based on these results, it is possible to affirm that the mass transportion of the electroactive species onto the electrode surface is preferentially diffusion-controlled. Curiously, this is a different behavior from that registered for artemisinin, in which the results had shown that the voltammetric reduction of the drug is controlled by adsorption [23]. In general, the product formed by the redox reaction adsorbs on the electrode. Eventually, the solubility differences between the drugs [9] could explain the contrast in behaviors on the electrode surface [36].

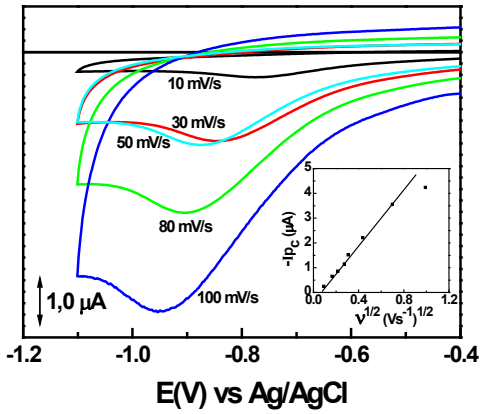

Figure 4. Cyclic voltamograms of 1.0 mmol L^{-1} of artesunate at pH = 6.0. Inset: linear dependence on the peak current with the scan rate square-root.

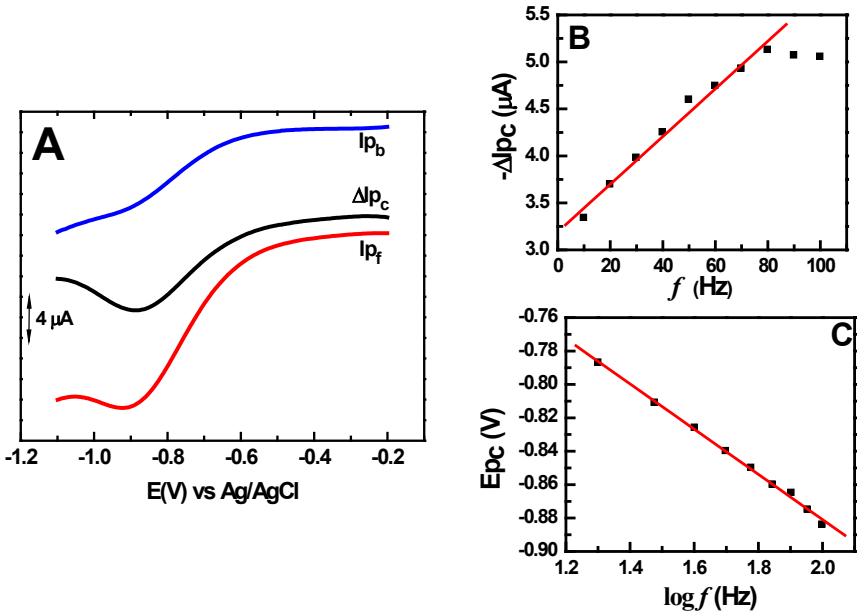

Figure 5. (A) Square wave voltammogram of 0.1 mmol L^{-1} of artesunate at pH = 6.0; (B) Plot of ΔIp_c *vs f*; (C) Plot of Ep_c *vs* log *f*.

Complementary data obtained by applying square wave voltammetry corroborate the results described above. Considering the following parameters: frequency (*f*) = 80 Hz; pulse amplitude (a) = 50.0 mV and sweeping increase (ΔEs) = 2.0 mV, at pH 6.0 one single cathodic peak was registered (-0.894 V) for artesunate. The voltammograms presented in Figure 5A show that the respective net currents (ΔIp_c) are composed only by the direct current (Ip_f), being the reverse current (Ip_b) absent, which indicates lack of backward component, confirming an irreversible system. According to literature [37, 38], the frequency for pulse application is an important parameter used in mechanistic and kinetic studies., for a system totally irreversible the ΔIp_c values vary linearly with frequency, as it can be observed in Figure 5B in which this proportionality occurs until 80 Hz. The net peak potential as a function of the logarithm of frequency provide related information regarding mass transportation phenomenon, indicating that the process involving a redox reaction may be controlled by either diffusion or adsorption of the product and/or reagent. Figure 5C shows the plot between Ep_c *vs* log *f,* being a linear correlation observed in the frequency range studied (20 Hz < *f* < 100 Hz), which confirms that the charge transfer process for the artesunate voltammetric reduction is controlled by diffusion.

Artesunate follows a similar voltammetric behavior in function of the pH value variations registered for artemisinin, by which the peak current values are pH-dependents, while the peak potential values are not shifted with the solution acidity change [23]. The Ep_c *vs.* pH plot in Figure 6 clearly shows this behavior described for artesunate. The pH effect was evaluated in the range 2 < pH < 12 with a total variation on the Ep_c values that did not reach to 0.1 V, showing that the reduction peak is kept constant in all pH range studied. However, it is possible to observe by the Ip_c *vs.* pH plot (Figure 6) that in acidic medium the Ip_c values suffer small influence of pH, but from pH = 6.0 there is an increase of the current values with the proton decrease in solution. These results demonstrate that the proton-equilibrium may occur after the electron transfer step and the reduction rate of artesunate is increased with pH [32].

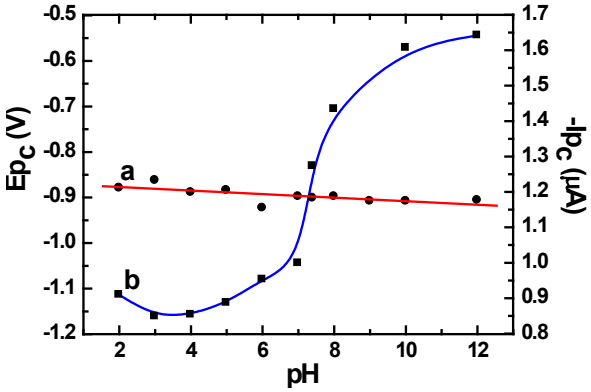

Figure 6. The evaluation of the pH influence: (a) Ep_c *vs.* pH and (b) Ip_c *vs.* pH. [Artesunate] = 1.0 mmol L^{-1}; ν = 0.1 V s^{-1}.

The knowledge of the number of electrons associated to an electrode reaction is essential for the better comprehension of the redox mechanism involving a drug. Thus, the number of electrons involved in the electrochemical reductions of artesunate and artemisinin were estimated at pH 7.4, considering the physiological pH as reference. From the electrolytic measurements at controlled potential, a curve relating the generated reduction current in function of the time is registered. For this chronoamperogram obtained, the Cottrell equation is valid [32].

$$I_d = \frac{nFAD^{1/2}C}{\pi^{1/2}t^{1/2}},$$

being I_d measured current (A), n is the number of electrons, A is the electrode area (cm^2), C is the initial concentration of drug (mol cm^{-3}), D is the diffusion coefficient of the solute in water(cm^2s^{-1}) and t is the time (s) and F (96,485 C mol^{-1}). Being the relationship between I_d in function of $t^{-1/2}$ linear, from its slope determined and having all the parameters known, the number of electrons can be calculated. Previous works [39, 40] have demonstrated that the application of chronoamperometry associated to the prediction of diffusion coefficient by molecular modeling is an efficient strategy for the number of electrons determination involved in the electrode reaction of drugs. Initially, the diffusion coefficient has been predicted by Wilke-Chang equation,

$$D = \frac{7.4 \times 10^{-8}(x\ M)^{0.5}T}{\eta^{0.6}\ V},$$

being D the diffusion coefficient of the solute in water (cm^2 s^{-1}); η is the viscosity of water

(centipoise) at the temperature of interest (η = 0.8937 at 25 °C), M is the molar mass of water (g mol^{-1}), T is the temperature (K), *x* is the association parameter (2.53) of water and V is the Le Bas molar volume of the solute (cm^3 mol^{-1}) [42]. This last one is an additive method for molar volume calculation from atomic contributions that make up the functional groups present in organic molecules [42]. Firstly, the molecular volume of the drugs (Table 1) were predicted by the AM1 molecular modeling semi-empirical method through the Molinspiration program (an internet free software) [41]; secondly, these obtained values were applied in the relationship previously established by La-Scalea *et al.* [42] and the respective Le Bas molar volumes were calculated. It is worth mentioning that Le Bas molar volumes correlate linearly with Van der Waals volumes, which is the basis of calculation for the AM1 semi-empirical method [42]. Thus, Figure 7A presents the chronoamperogram obtained for the artesunate following the parameters as already described. The Cottrell linear relationship showed excellent correlation (R^2 = 0.998) as it can be observed in Figure 7B and the results from the electrolytic reduction of artemisin and artesunate are presented on Table 1. It is evident the concordance of results for both drugs, demonstrating clearly the involvement of two electrons in the reduction electrochemical process.

Table 1. Number of electrons involved in the process calculated with the chronoamperometric data at pH 7.4

Drugs	Molecular volume (Å^3)	Diffusion coefficient (cm^2/s)	Cottrell slope (A/s^{½})*	n*
Artemisin	258.22	5.74x10^{-6}	4.7 ± 0.5x10^{-6}	1.9 ± 0.2
Artesunate	344.64	4.83x10^{-6}	4.4 ± 0.8x10^{-6}	1.9 ± 0.4

*average values from five measurements.

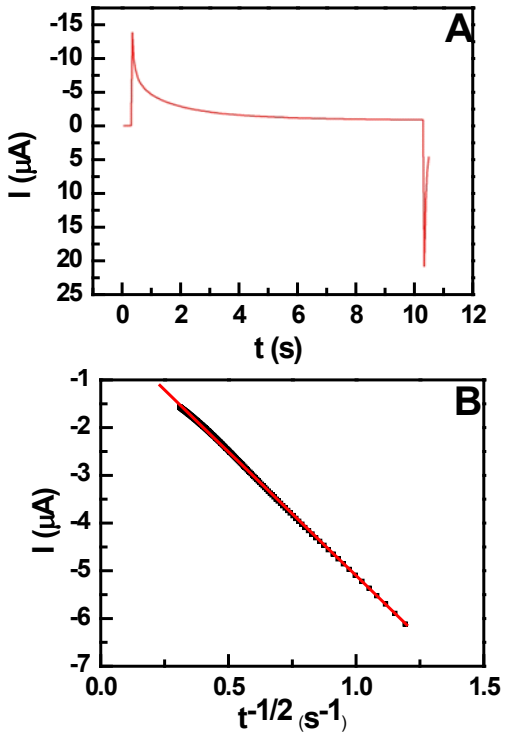

Figure 7. (A) Chronoamperogram of 1.0 mmol L^{-1} artesunate with applied potential at-0,9 V by 10 seconds; (B) Plot of I_d *vs.* $t^{-1/2}$.

Complementing the electrochemical studies of the artesunate, a molecular modeling approach was carried out in order to contribute towards a better comprehension of the reduction mechanism. In this sense, the molecular modeling methodology enables the determination of the frontier molecular orbitals involved in the redox process electrons flow. When an oxidation reaction occurs, the electron from the highest occupied molecular orbital (HOMO) is transferred, while for a reduction process the electron flows from the electrode into the lowest unoccupied molecular orbital (LUMO) of the studied molecule. Concerning the obtained results, it can be affirmed that the reduction mechanism of artesunate is the same of artemisinin, indicating that the endoperoxide bridge is broken with the respective formation of the diol-derivative that leads to the consequent stability of the deoxy analog [9, 48], involving a total of 2e/2H$^+$. The calculations were performed considering the artesunate molecular structure (ground state) and two more molecular states (derivate 1 and derivate 2), taking in to account the possible products formed in the drug voltammetric reduction. The structures of the three compounds were obtained from a conformational search using molecular mechanics. Geometry optimization was then

performed at the DFT (B3LYP/6-311 + G(d,p)) level of theory. The geometry optimized for each of the studied forms is shown in Figure 8.

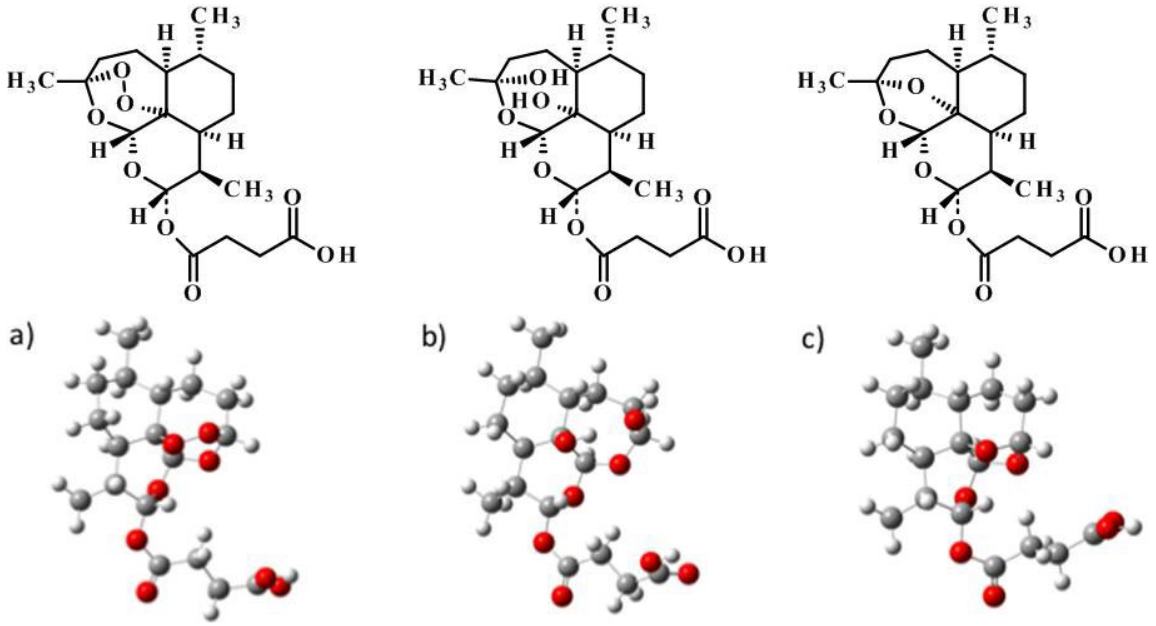

Figure 8. Structures optimized for the molecular modeling study: a) ground state (artesunate); b) derivative 1 (diol-derivative) and c) derivative 2 (deoxy analog).

The results obtained indicate that the LUMO orbitals, which will be the easiest route to the addition of electrons to the molecule, are located around the conjugated rings (artesunate and derivate 1) and they are dislocated to the lateral chain, considering the derivate 2 formed after the electrons transfer (Figure 9). These results for the artesunate corroborate those registered in literature suggesting that the deoxy analog is not involved in the action drug because this molecule is more stable than the endoperoxide group and the hydroxyl groups formed to the derivative 1 [43].

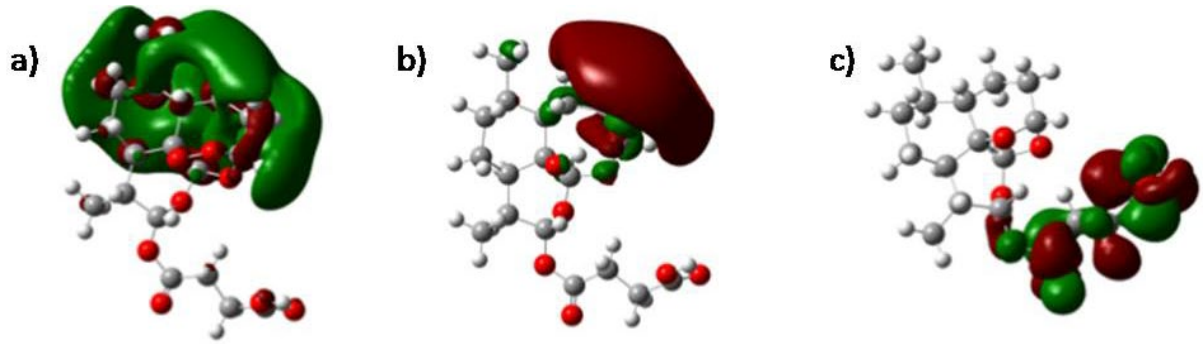

Figure 9. Results obtained by molecular modeling studies for LUMO orbitals, showing the differences and changes for a) artesunate; b) derivate 1 and c) derivate 2.

Based on the literature data [9, 23, 43] and the results herein discussed, it is possible to suggest a sequence that presents a set of reactions involving protonation and charge transfer steps, being defined e^-, H^+, e^-, H^+, as depicted in Scheme 1.

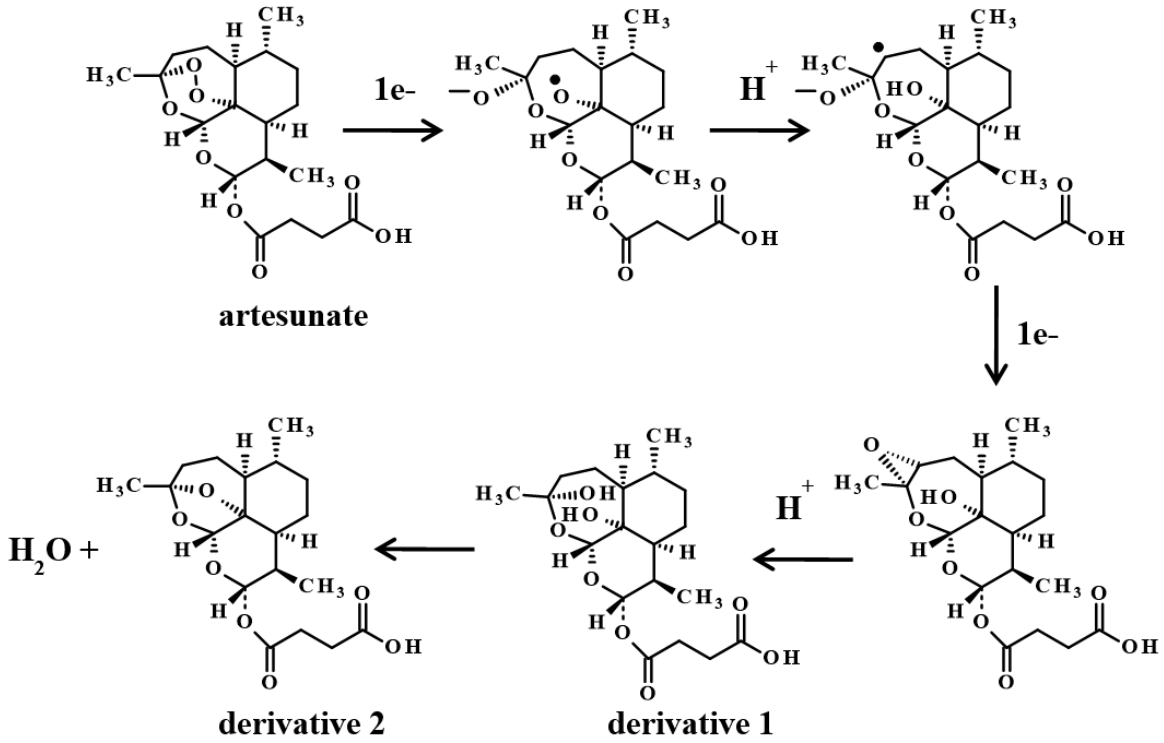

Scheme 1. Reduction mechanism proposed for the artesunate on GCE.

3. Material and Methods

3.1 Reagents and solutions

The stock solutions (0.05 mol L^{-1}) of artemisinin (Medyplantex) and artesunate (Farmanguinhos/Fiocruz) were prepared through direct dissolution in methanol. The solution of $K_3Fe(CN)_6.3H_2O$ (0.01 mol L^{-1}) was prepared in water. The pH study of the final drug solution was accomplished with Britton-Robison (BR) universal buffer [44]. All solutions were prepared by using analytical-grade reagents from Merck and ultrapure water from a Gehaka UV system.

3.2 Apparatus

The electrochemical measurements were carried out using an Autolab PGSTAT 30 potentiostat/galvanostat from Eco-Chimie, Utrecht, Netherlands, coupled to a 20 mL cell with a three-electrode system, being glassy carbon as the working electrode (GCE) and the other two, Ag/AgCl as the reference and Pt as auxiliary. The acquisition and treatment of data were performed using the GPES 4.9 program (Eco-Chimie). Dissolved air was removed from the solutions by 10 min bubbling with nitrogen. The pH control was measured with a Metrohm 654-pH-meter and the combined glass electrode at room temperature.

The GCE (∅ = 2 mm, Analion, Brazil) was manually polished with 1 μm diamond suspension in spray on Supra metallographic velvet (Arotec S/A, granulometry ¼ μm). The GCE was rinsed with ultrapure water after having been polished. The GCE area (0.0189 ± 0.002 cm^2) was determined from cyclic voltammetry data obtained for $K_3Fe(CN)_6.3H_2O$ and its diffusion coefficient ($7.76x10^{-6}$ cm^2 s^{-1}) in KCl 0.5 mol L^{-1} solution and applying the Randles-Ševcik equation for the reversible system $[Fe(CN)_6]^{3-}/[Fe(CN)_6]^{4-}$[32].

3.3 Electrochemical assays and the determination of the number of electrons

The electrochemical behavior of artesunate (1.0 mmol L^{-1}) in BR buffer was analyzed using the cyclic voltammetry in the scan range from -0.2 to 1.2 V *vs.* Ag/AgCl reference electrode and the scan rate varied from 10 to 1000 mV s^{-1}, having artemisinin as reference compound in the same experimental conditions. All the voltammetric measurements were carried out after bubbling nitrogen during 10 minutes.

The number of electrons was determined at pH 7.4 with drug concentration of 0.1 mmol $L^{-1}$by

chronoamperometry using three levels of potential pulses. Level 1: potential 0 V, duration 0.3 s, sampling time 0.05 s. Level 2: potential -0.9 V, duration 10 s, sampling time 0.05 s. Level 3: potential 0 V, duration 0.2 s, sampling time 0.05 s. From the chronoamperograms registered, the linear relation between I_d as a function of $t^{-1/2}$ was plotted based on Cottrell equation [32].

The diffusion coefficient predictions of the studied compounds in aqueous phase with infinite dilution were carried out following methodology reported elsewhere [42], in which the Wilke-Chang equation was applied by using the molecular volume data calculated by the online internet free software with input of SMILES strings for artemisinin and artesunate [41].

3.4 Computational methodology

The computational studies consisted of (i) constructing the 3D structures, (ii) performing a conformational search employing the MMFF94 classical force field [45] by systematic sampling using the Spartan'10 software (iii) geometry optimization, (iv) calculating imaginary frequencies, and (v) performing density functional theory (DFT) calculations to determine electronic properties using the B3LYP functional and 6-311 + G (d,p) implemented in the Gaussian 03 package [46]. Several structural and electronic properties were calculated from the DFT calculations, such as molecular orbital (MO) energies [47, 48].

4. Conclusions

Artesunate was irreversibly reduced by a diffusion-controlled process on the glassy carbon electrode in aqueous media by using cyclic voltammetry. Only one wave was registered, being its peak potential value shifted to the negative potential values with the scan rate increased and independent of the pH. However, the cathodic current value increased its magnitude in alkaline media, indicating that the proton-equilibrium may occur after the electron transfer process. From the chronoamperometric data, two electrons were determined for the reduction of artesunate and artemisinin, confirming that both drugs have the same redox process. The computational approach reinforced that the artesunate reduction mechanism involves the breakage of the endoperoxide bridge and consequent diol-derivative formation followed by the deoxy analog stabilization, which corroborates the idea that the endoperoxide group is responsible for the drug action. The general discussion of this work indicates that the artesunate reduction mechanism involves the possible existence of a set of reactions involving protonation and charge transfer steps on the electrode surface.

References

[1] Available from: http://www.who.int/topics/malaria/en. Accessed January, 2018.

[2] Trouiller, P.; Torreele, E.; Olliaro, P.; White, N.; Foster, S.; Wirth, D.; Pécoul, B. *Trop. Med. Int. Health* **2001**, *6*, 945. [Crossref]

[3] Dimitri, N. *Plos One* **2012**, *7*, e50835. [Crossref]

[4] Johnston, K. L.; Ford, L.; Taylor, M. J. *J. Biomol. Screening* **2014**, *19*, 335. [Crossref]

[5] Mrazek, M. F.; Mossialos, E. *Health Policy* **2003**, *64*, 75. [Crossref]

[6] Juliano, R. L. *Science and Public Policy* **2013**, *40*, 393. [Crossref]

[7] Wells, S.; Diap, G.; Kiechel, J. R. *Malar. J.* **2013**, *12*, 3. [Crossref]

[8] Varotti, F. P.; Botelho, A. C. C.; Andrade, A. A.; Paula, R. C.; Fagundes, E. M. S.; Valverde, A.; Mayer, L. M. U.; Mendonça, J. S.; Souza, M. V. N.; Krettli, A. U. *Antimicrob. Agents Chemother.* **2008**, *52*, 3868. [Crossref]

[9] Ansari, M. T.; Saify, Z. S.; Sultana, N.; Ahmadi, I.; Saeed-Ul-Hassan, S.; Tariq, I.; Khanums, M. *Mini-Rev. Med. Chem.* **2013**, *13*, 1879. [Crossref]

[10] Dassonville-Klimprt, A.; Jonet, A.; Pillon, M.; Mullié, C.; Sonnet, P. In: Science Against Microbial Pathogens: Communicating Current Research and Technological Advances, Méndez-Vilas, A., ed. Badajoz: Formatex Research Center, 2011, volume 3, chapter 1.

[11] Hood, J. E.; Jenkins, J. W.; Milatovic, D.; Rongzhu, L.; Aschner, M. *Neurotoxicology* **2010**, 31, 518. [Crosrref]

[12] Abreu, F. C.; Moura, M. A. B. F.; Ferreira, D. C. M.; Cavalcanti, J. C. M.; Goulart, M. O. F. In: Química Medicinal. Métodos e Fundamentos em Planejamento de Fármacos. Montanari, C. A., ed. São Paulo: Edusp, 2010, chapter 6.

[13] Álvarez-Lueje, A.; Pérez, M.; Zapata, C. In: *Topics on Drug Metabolism*. Paxton, J., ed. Rijeka: Intech, 2012, chapter 9.

[14] Almeida, M. O.; Maltarollo, V. G.; De Toledo, R. A.; Shim, H.; Santos, M. C.; Honorio, K. M. *Curr. Med. Chem.* **2014**, *21*, 2266. [Crossref]

[15] Wu, W. M.; Wu, Y. L *J. Chem. Soc., Perkin Trans. 1* **2000**, *24*, 4279. [Crossref]

[16] Zhang, F.; Gosser Jr., D. K.; Meshinick, S. R. *Biochem. Pharmacol.* **1992**, *43*, 1805. [Crossref]

[17] Jiang, H. L.; Chen, K. C.; Tang, Y.; Chen, J. Z.; Li, Y.; Wang, Q. M.; Ji, R. Y. *Indian J. Chem., Sect. B: Org. Chem. Incl. Med. Chem.* **1997**, *36*, 154.

[18] Donkers, R. L.; Workentin, M. S. *The Journal of Physical Chemistry B*, **1998**, *102*, 4061. [Crossref]

[19] Chen, Y.; Zheng, J. M.; Zhu, S. M.; Chen, H. Y. *Electrochim. Acta* **1999**, *44*, 2345. [Crossref]

[20] Chen, Y.; Zhu, S. M.; Chen, H. Y.; Li, Y. *Bioelectrochem. Bioenerg.* **1998,** *44*, 295. [Crossref]

[21] Yang, P. H.; Zhou, Z. J.; Cai, J. Y. *Colloids Surf., A* **2005**, *257-258*, 467. [Crossref]

[22] Yang, X.; Gan, T.; Zheng, X.; Zhu, D.; Wu, K. *Bull. Korean Chem. Soc.* **2008**, *29*, 1386. [Crossref]

[23] La-Scalea, M. A.; Silva, H. S. R. C.; Ferreira, E. I. *Rev. Bras. Cienc. Farm.* **2007**, *43*, 371. [Crossref]

[24] Mugweru, A. M.; Shoe, A.; Kahi, H. K.; Kamau, G. N. *Int. J. Chem. Kinet.* **2016**, *48*, 72. [Crossref]

[25] Bhattacharjee, A. K.; Skanchy, D. J.; Hicks, R. P.; Carvalho, K. A.; Chmurny, G. N.; Klose, J. R.; Scovill, J. P. *Internet Electron. J. Mol. Des.* **2004**, 3, 55. [Link]

[26] Debnath, C.; Haslinger, E.; Likussar, W.; Michelistsch, A. *J. Pharm. Biomed. Anal.* **2006**, *41*, 638. [Crossref]

[27] Jain, R.; Vikas. *Colloids Surf., B* **2011**, *88*, 729. [Crossref]

[28] Sibmooh, N.; Udomsanogpetch, R.; Kijom A.; Chantharaksri, U.; Mankhertkotn, S. *Chem. Pharm. Bull.* **2001**, *49*, 1541. [Crossref]

[29] Cai, H. H.; Cai, J.; Yang, P. H. *Bioorg. Med. Chem. Lett.* **2009**, *19*, 863. [Crossref]

[30] Cai, H. H.; Yang, P. H.; Cai, J. Y. *J. Electroanal. Chem.* **2008**, *619-620*, 59. [Crossref]

[31] Mazzochette, Z.; Newton, E.; Mugweru, A. *Anal. Methods* **2017**, *20*, 2971. [Crossref]

[32] Bard, A. J.; Faulkener, L. R. Electrochemical Methods. Fundamentals and Applications, 2nd ed. Hoboken: John Wiley and Sons, 2001.

[33] Nikodimos, Y.; Amare, M. *J. Anal. Methods Chem.* **2016**, *ID 3612943*, 1. [Crossref]

[34] Fotouhi, L.; Fatollahzadeh, M.; Heravi, M. M. *Int. J. Electrochem. Sci.* **2012**, *7*, 3919. [Crossref]

[35] Gosser Jr, D. K. Cyclic voltammetry. Simulation and analysis of reaction mechanisms. New York: VCH, 1993.

[36] Srinivasan, S. In: Fuel cells. From fundamentals to applications. Srinivasan, S., ed. Boston: Springer, 2006, chapter 2. [Crossref]

[37] de Souza, D.; Codgnoto, L.; Malagutti, A. R., Toledo, R. A.; Pedrosa, V. A.; Oliveira, R. T. S.; Mazo, L. H.; Avaca, L. A.; Machado, S. A. S. *Quim. Nova* **2003**, *26*, 81. [Crossref]

[38] Mirceski, V.; Komorsky-Lovric, S.; Lovric, M. Berlin: Springer, Square-Wave Voltammetry, 2007. [Crossref]

[39] Brito, C. L.; Trossini, G. H. G.; Ferreira, E. I.; La-Scalea, M. A. *J. Braz. Chem. Soc.* **2013**, *24*, 1964. [Crossref]

[40] Miyano, D. M.; Lima, T.; Simões, F. R.; La-Scalea, M. A.; Oliveira, H. P. M.; Codognoto, L. *J. Braz. Chem. Soc.* **2014**, *25*, 602. [Crossref]

[41] Available from: http://www.molinspiration.com. Accessed December, 2016.

[42] La-Scalea, M. A.; Menezes, C. M. S.; Ferreira, E. I. *J. Mol. Struct.: THEOCHEM* **2005**, *730*, 111. [Crossref]

[43] Taranto, A. G.; Carneiro, J. W. M.; Araujo, M. T. *Bioorg. Med. Chem.* **2006**, *14*, 1546. [Crossref]

[44] Lurie, J. *Handbook of Analytical Chemistry*. Moscow: Mir, 1978.

[45] Halgbren, T. A. *J. Comput. Chem.* **1996**, *17*, 490. [Crossref]

[46] Frisch, M. J.; Trucks, G. W.; Schkegek, H.B.; Scuseria, G. E.; Robb, M. A.; Chessman, J. R.; Montgomery Jr, J. A.; Vreven, T.; Kudin, K. N.; Burant, J. C.; Millam, J. M.; Iyengar, S. S.; Tomasi, J.; Barone, V.; Mennucci, B.; Cossi, M.; Scalmani, G.; Rega, N.; Petersson, G. A.; Nakatysuji, H.; Hadam, E. M.; Toyota, K.; Fukuda, R.; Hasegawa, J.; Ishida, M.; Nakajima, T.; Honda, Y.; Kitao, O.; Nakai, H.; Klene, M.; Li, X.; Knox, J. E.; Hratchian, H. P.; Cross, J. B.; Bakken, V.; Adam, C.; Jaramillo, J.; Gomperts, R.; Stramann, R. E.; Yazyev, O.; Austin, A. J.; Cammi, C. Pomelli, J.W. Ochterski, P. Y. Ayala, K. Morokuma, G. A. Voth, P. Salvador, J. J. Dannenberg, R.; Zakrzewski, V. G.; Dapprich, S.; Daniels, A. D.; Strain, M. C.; Farkas, O.; Malick, D. K.; Rabuck, A. D.; Raghavachari, K.; Foresman, J. B.; Ortiz, J. V.; Cui, Q.; Baboul, A. G.; Clifford, S.; Cioslowski, J.; Stefanov, B. B.; Liu, G.; Liashenko, A.; Piskorz, P.; Komaromil, I.; Martin, R. L.; Fox, D. J.; Keith, T.; Al-Laham, M. A.; Peng, C.Y.; Nanayakkara, A.; Challacombe, M.; Gill, P. M. W.; Johnsons, B.; Chen, W.; Wong, M. W.; Gonzalez, C.; Pople J. A. *Gaussian 03*, Wallingford: Gaussian Inc, 2004.

[47] Garcia, R. D.; Maltarollo, V. G.; Honorio, K. M.; Trossini, G. H. G. *J. Mol. Model.* **2015**, *21*, 1. [Crossref]

[48] Trossini, G. H. G.; Maltarollo, V. G.; Gargia, R. D.; Pinto, C. A. S. O.; Velasco, M. V. R.; Baby, A. R. *J. Mol. Model.* **2015**, *21*, 1. [Crossref]